

Rheoviscometry of Offset Inks and their Emulsions with Water

J. KINDERNAY, J. PANÁK, and M. MIKULA

*Department of Graphic Arts Technology and Applied Photochemistry,
Faculty of Chemical Technology, Slovak University of Technology,
SK-812 37 Bratislava
e-mail: kinderna@chelin.chtf.stuba.sk*

Received 21 December 1999

A stress-controlled rheometer with cone and plate geometry was used to study the rheological properties of four sets of process offset inks and their emulsions with low water content. All systems have shown typical pseudoplastic shear-thinning behaviour. Because of some measuring problems concerning a remounting of inks from measuring gap, the flow curve was properly segmented and the optimal measuring interval ΔD_{opt} was defined. The Ostwald flow model was chosen as the best from three applied mathematical models. Finally, the quantitative flow parameters were calculated and discussed in connection with ink press performance.

The offset printing is based on the ink transport from an ink reservoir and ductor through a system of inking rollers to a form cylinder and through blanket of an offset cylinder onto a substrate – usually paper. During the various stages of printing, a printing ink experiences a very wide range of compressional, shear, and extensional deformations. Therefore, the ink transport is influenced especially by its rheological properties. The rheological properties are, besides another, backward influenced also by its transport. The image and nonimage areas of the printing plate are on the same plane. The selective transport of ink only by image areas requires presence of thin layer of the fountain solution on the nonimage areas. The layers of the fountain solution and ink are deposited during one turnover (at the same time) on the image and nonimage area of the offset roller, respectively.

Offset printing inks are based on suspensions of solid pigment particles (15–25 mass %) in liquid vehicle. Pigment particles are solid colouring agents, dispersed in vehicle, and that is nondissolving also in water and organic solvents. As for rheological properties the vehicle is the most important part of ink. The main role of the vehicle is to guarantee transport behaviour of an ink in printing machine and to perform the pigment binding on the printed material surface. Offset inks differ in viscosity and in the manner and rate of drying, in connection with the used technological conditions, printing speed, and substrates.

The offset printing process is characterized by emulsification of the fountain solution in the ink. The fountain solution is a dilute aqueous solution of several functionalized agents with pH in the range from 4 to 6, approximately. The optimal technological ink–water emulsion includes 8 to 25 mass % of fountain solu-

tion. During the stable printing process the dynamic steady state and the constant water content in the ink is achieved. Every ink has its own ability of receiving the fountain solution called “emulsification capacity” [1–4]. Several authors have described surprising phenomenon of increasing (or alternating) emulsion viscosity value due to the rising of water content [5–7]. The flow properties of emulsions significantly depend on the type of fountain solution, which was studied and described before [2, 4, 5, 7].

There are very high values of operating speed achieved during the press process whereas the laboratory measurements are limited by existence of critical shear rate. The appearance of critical shear rate is caused by the so-called “Weissenberg effect”, which is characterized by remounting of the ink from the measuring gap of cone/plate system. This problem is related especially to the emulsion measurements, because of a high sensitivity of emulsions to a preparation procedure. The preparation arrangement with the effect of different factors on the emulsion process preparation and optimization is described by *Surland* [2].

The aim of this work is to study the flow curves of ink–water emulsions and the water content effect on rheology of offset inks. Furthermore, the aim is to analyze and separate particular segments of flow curves, to describe them with reference to measurement reproducibility and their applicability for modeling of rheological behaviour using different mathematical models.

EXPERIMENTAL

In connection with different offset techniques,

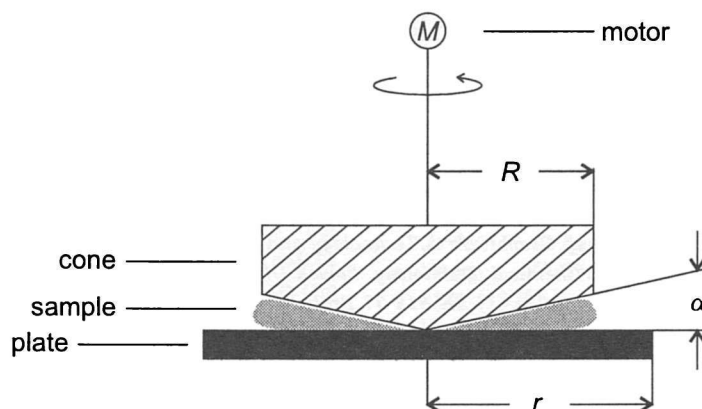


Fig. 1. Cone/plate geometry.

printing, and drying rates we chose four representative process inks. We tested all four process inks (C – cyan, M – magenta, Y – yellow, K – black). The inks were obtained from commercial producers: *Newsinks* (SCHMIDT DRUCKFARBEN; 45E (C), 35E (M), 25E (Y), 85E (B)/9880), *Heatset inks* (MICHAEL HUBER; 56 3030 (C), 56 2030 (M), 56 1030 (Y)/55, 66 7030 (K)/56), *Sheetfed inks – Rapida* (MICHAEL HUBER; 43 FW, 42 FW, 41 FW, 49 FW/7000), *Sheetfed inks – Reflecta* (MICHAEL HUBER; 43 F, 42 F, 41 F, 49 F/8550).

Instead of commercially manufactured fountain solution we used distilled water.

The rheological measurements were performed using a control-rate rheometer VISCOTESTER VT 500 made by HAAKE Mess-Technik GmbH (Germany) with cone and plate geometry illustrated in Fig. 1, with the parameters: cone radius, $R = 7.5$ mm, plate radius, $r = 15$ mm, cone angle, $\alpha = 1.6^\circ$.

All rheological measurements were realized at $(25 \pm 0.2)^\circ\text{C}$ with sample volume of ink approximately 130 mm^3 . At first we made measurements in full scale of D (far from D_{crit}). So we achieved attributes of parameters D_{min} , D_{max} , D_{crit} . The meaning of these parameters is clear from Fig. 2. Time of measurements was 4 min. The rheological measurements of 10 mass % and 20 mass % emulsions were made, too, for each ink sample. Emulsions were prepared by mixing of 22.5 g of the ink and 2.5 g of distilled water (for 10 mass % emulsions of water in the ink) or 20 g of the ink and 5 g of distilled water for 20 % emulsions, respectively. The operating speed of the blade stirrer with 2 blades was kept in scale of $(380 \pm 40) \text{ min}^{-1}$. This process takes 20 min. The temperature of the system was kept at $(25 \pm 2)^\circ\text{C}$.

The measurement allows to determine the shear stress τ as a function of shear rate D (flow curve), or the apparent viscosity η as a function of shear rate (viscosity curve).

The equipment-dependent flow curve alone (or viscosity curve) provides only a qualitative comparison between inks. It is essential to describe flow behaviour

of inks quantitatively, using a model. Many model equations have been reported in the literature to fit the experimental data.

The description of flow behaviour and rheological properties of analyzed inks was performed using mathematical models that were found to be suitable to interpret the measured data in the region ΔD between D_{min} and D_{max} . The various mathematical models were used.

Ostwald model:

$$\tau = k^* \cdot D^n$$

where n is the exponent characterizing the flow properties of inks ($n = 1$ for Newtonian liquids, $n > 1$ for dilatant liquids, and $n < 1$ for pseudoplastic liquids). Parameter k^* represents consistency of the ink and it is related to η .

Casson model:

$$\tau^{1/2} = \tau_d^{1/2} + (k^*)^{1/2} \cdot D^{1/2}$$

where τ_d is dynamic yield stress. The meaning of parameter k^* is the same as in the Ostwald model.

Logarithmic model:

$$\log\{\eta\} = \log\{\eta_0\} + (n - 1) \cdot \log\{D\}$$

where η_0 is the viscosity at $D = 1 \text{ s}^{-1}$.

Tables of processed data include values of the hysteresis loop area A (in Pa s^{-1}) measured in the range of D from 110 s^{-1} to 190 s^{-1} , $\eta(D = 60 \text{ s}^{-1})$ or $\eta(D = 120 \text{ s}^{-1})$ and the results of mathematical models analysis with the values of parameters, their deviations, and correlation coefficient K_k .

RESULTS AND DISCUSSION

As seen from Fig. 2, the flow curve could be segmented into four parts:

$D_0 - D_{\text{min}}$ is a region of unsteady flow behaviour. It is caused by unstable slipping of more or less amount

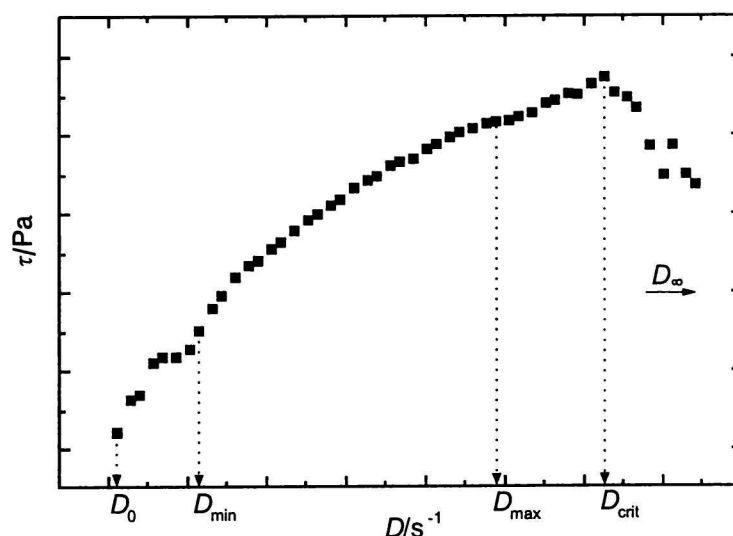


Fig. 2. Segmentation of the flow curve.

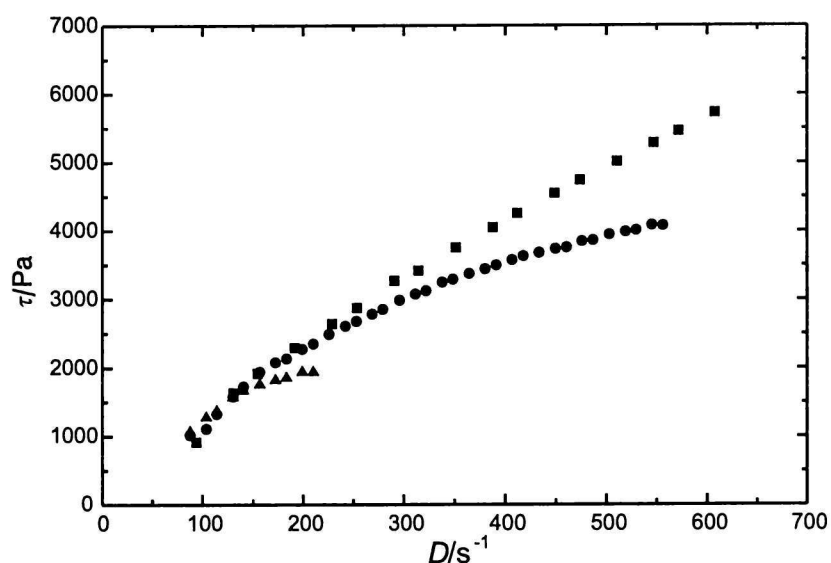


Fig. 3. Steady flow region of the flow curves of yellow newsink (square) and its 10 mass % (circle) and 20 mass % (up triangle) emulsions.

of analyzed inks in the cone/plate system or by higher limit of used device sensitivity for given sensorial system cone/plate.

D_{\min} – D_{\max} is a region of steady flow of the ink. This region is suitable for application of mathematical models. It is characterized by steady slope of the flow curve.

D_{\max} – D_{crit} is a region characterized by the change of the flow curve slope that is not related only to non-Newtonian behaviour. It is a transitional area between regular and nonregular (nonreproducible) part of the flow curve.

D_{crit} – D_{∞} is a region of nonregular measurement unsuitable for modeling of flow properties of analyzed samples. Sharp and nonmonotonous decreasing of the flow curve in the region is due to “Weissenberg effect”. This effect resides in the ink remounting from measuring gap of the cone/plate system at higher values of D ,

which is caused by migration of ink as non-Newtonian liquid to a place with lower shear, *i.e.* lower shear rate.

As seen from Fig. 3, the steady flow region is significantly reduced by increasing of water content. It is caused by worse stability of the ink emulsions in comparison with pure inks or low-water-content emulsions. At higher levels of fountain solution and as the rate of shear increased, the dispersed fountain solution eventually coalesces into water droplets. So in the case of nonstable systems, due to the lack of emulsion stability, the critical structure breakdown point (τ_{crit}) is shifted to a much lower shear rate value with each additional level of fountain solution.

Web-offset printing is done basically with two types of printing ink: coldset or news inks and heatset inks. Both must be formulated to fulfil the requirements of high press speed and fast drying. Since heatset inks are used for higher-quality publication print-

Table 1. Results of Newsinks Flow Curve Segmentation, Thixotropy Measurement, and the Application of the Mathematical Models

Newsinks	$w(\text{water})$	D_{\min}	D_{\max}	D_{crit}	A	$\eta(D = 60 \text{ s}^{-1})$	Ostwald	$\{P\}$	Logarithm	$\{P\}$	Casson	$\{P\}$
	%	s^{-1}	s^{-1}	s^{-1}	$\text{Pa s}^{-1} 10^{-4}$	Pa s						
C	0	106	467	514	0.5890	20.37	136 ± 9	$\{k^*\}$	858 ± 1	$\{\eta_0\}$	676 ± 1	$\{\tau_d\}$
	10	94	210	252	2.3189	21.72	0.63 ± 0.01	n	0.53 ± 0.01	n	6.29 ± 0.01	$\{k^*\}$
	20	99	135	143	13.4801	18.91	0.9973	K_k	0.9997	K_k	0.9787	K_k
M	0	97	200	221	1.5239	22.23	88 ± 13	$\{k^*\}$	102 ± 4	$\{\eta_0\}$	219 ± 3	$\{\tau_d\}$
	10	97	186	221	2.6929	16.21	0.74 ± 0.03	n	0.70 ± 0.03	n	13.2 ± 0.03	$\{k^*\}$
	20	99	138	144	4.0082	11.73	0.9997	K_k	0.9997	K_k	0.9980	K_k
Y	0	90	1340	1345	0.1525	12.35	43 ± 1	$\{k^*\}$	41 ± 1	$\{\eta_0\}$	232 ± 0.3	$\{\tau_d\}$
	10	90	558	588	0.5494	11.83	0.76 ± 0.01	n	0.77 ± 0.01	n	6 ± 0.001	$\{k^*\}$
	20	90	210	—	1.2550	10.31	0.9978	K_k	0.9967	K_k	0.9720	K_k
K	0	99	240	250	0.9702	16.84	123 ± 8	$\{k^*\}$	124 ± 1	$\{\eta_0\}$	489 ± 0.66	$\{\tau_d\}$
	10	99	143	182	1.2640	16.67	0.61 ± 0.01	n	0.61 ± 0.01	n	5.5 ± 0.002	$\{k^*\}$
	20	99	135	134	5.3423	14.44	0.9996	K_k	0.9996	K_k	0.9972	K_k

Table 2. Results of Heatset Inks Flow Curve Segmentation, Thixotropy Measurement, and the Application of the Mathematical Models

Heatset inks	$w(\text{water})$	D_{\min}	D_{\max}	D_{crit}	A	$\eta(D = 120 \text{ s}^{-1})$	Ostwald	$\{P\}$	Logarithm	$\{P\}$	Casson	$\{P\}$
	%	s^{-1}	s^{-1}	s^{-1}	$\text{Pa s}^{-1} 10^{-4}$	Pa s						
C	0	100	190	224	2.7914	32.79	53 ± 4	$\{k^*\}$	51 ± 1	$\{\eta_0\}$	40.5 ± 0.88	$\{\tau_d\}$
	10	92	170	185	3.3282	31.75	0.89 ± 0.02	n	0.90 ± 0.02	n	26 ± 0.007	$\{k^*\}$
	20	92	133	140	14.8743	33.74	0.9994	K_k	0.9994	K_k	0.9994	K_k
M	0	100	184	193	2.0145	27.77	67 ± 7	$\{k^*\}$	65 ± 1	$\{\eta_0\}$	112.3 ± 1.7	$\{\tau_d\}$
	10	92	156	156	2.6339	17.06	0.82 ± 0.02	n	0.83 ± 0.02	n	19 ± 0.013	$\{k^*\}$
	20	—	—	—	2.6410	14.13	0.9997	K_k	0.9997	K_k	0.9997	K_k
Y	0	100	300	409	1.2875	20.83	86 ± 2	$\{k^*\}$	87 ± 1	$\{\eta_0\}$	332 ± 0.03	$\{\tau_d\}$
	10	100	200	588	3.6264	15.72	0.71 ± 0.01	n	0.71 ± 0.01	n	9.2 ± 0.001	$\{k^*\}$
	20	100	135	—	2.8796	12.66	0.9988	K_k	0.9987	K_k	0.9988	K_k
K	0	94	298	325	1.2494	14.62	74 ± 2	$\{k^*\}$	74 ± 1	$\{\eta_0\}$	274 ± 0.12	$\{\tau_d\}$
	10	99	165	185	0.0229	17.81	0.69 ± 0.01	n	0.70 ± 0.01	n	7.1 ± 0.001	$\{k^*\}$
	20	100	161	165	2.0034	22.76	0.9991	K_k	0.9990	K_k	0.9991	K_k

ing, the vehicle components must be chosen with care and known in detail [8].

Heatset offset inks have a relatively large content of solvents (almost 50 %) considering that they dry primarily by evaporation as the web goes through a hot-air dryer. Heatset inks are formulated on the basis of rosin-modified phenolic resin and high-boiling aliphatic petroleum distillates. Phenolic resins are available in low- and high-molecular mass modifications and in different solubilities. Petroleum distillates are used with boiling ranges of 240–270 °C and 260–290 °C. The pigment content is about 15–20 mass % [9], and other resins, solvents, and additives such as alkyd resins, fillers, and particularly waxes can also be included. In accordance with expectation the viscosity values of heatset inks assigned for high press

speed and fast drying need to be higher than the viscosity of newsinks (see Tables 1–4). As the sheetfed inks Rapida are specially designed for extremely high rates of drying, their $\eta(D = 120 \text{ s}^{-1})$ are higher than viscosity of heatset inks and even higher than $\eta(D = 60 \text{ s}^{-1})$ of newsinks. The values of $\eta(D = 60 \text{ s}^{-1})$ or $D = 120 \text{ s}^{-1})$ were mostly growing with the water content.

The D_{crit} parameter values varied from 221 to 1345 s^{-1} for newsinks, from 193 to 409 s^{-1} for heatset inks, from 146 to 258 s^{-1} for sheetfed inks Reflecta, and from 83 to 240 s^{-1} for sheetfed inks Rapida.

The result of the above-mentioned Weissenberg phenomenon was reduction of measurable scale to the scale from D_{\min} to D_{\max} (ΔD_{opt}). This range decreases with increasing of the system consistency and

Table 3. Results of Sheetfed Inks Reflecta Flow Curve Segmentation, Thixotropy Measurement, and the Application of the Mathematical Models

Reflecta	$w(\text{water})$	D_{\min}	D_{\max}	D_{crit}	A	$\eta(D = 60 \text{ s}^{-1})$	Ostwald	$\{P\}$	Logarithm	$\{P\}$	Casson	$\{P\}$
	%	s^{-1}	s^{-1}	s^{-1}	$\text{Pa s}^{-1} 10^{-4}$	Pa s						
C	0	13	130	146	10.1860	53.21	138 ± 11.2	$\{k^*\}$	123 ± 1	$\{\eta_0\}$	103.9 ± 0.8	$\{\tau_d\}$
	10	11	141	145	10.3782	41.52	0.77 ± 0.02	n	0.80 ± 0.02	n	36 ± 0.020	$\{k^*\}$
	20	11	71	87	9.3142	42.31	0.9908	K_k	0.9877	K_k	0.9407	K_k
M	0	10	66	209	12.0512	55.85	100 ± 13.0	$\{k^*\}$	95 ± 1	$\{\eta_0\}$	40.9 ± 1.8	$\{\tau_d\}$
	10	10	64	85	10.6374	41.15	0.88 ± 0.04	n	0.90 ± 0.02	n	49 ± 0.060	$\{k^*\}$
	20	10	64	75	8.3200	40.89	0.9916	K_k	0.9912	K_k	0.9533	K_k
Y	0	16	233	258	1.6017	40.41	79 ± 9.44	$\{k^*\}$	103 ± 1	$\{\eta_0\}$	133 ± 2.9	$\{\tau_d\}$
	10	16	210	242	1.8988	28.46	0.81 ± 0.02	n	0.76 ± 0.02	n	21 ± 0.020	$\{k^*\}$
	20	16	162	186	3.3025	24.22	0.9988	K_k	0.9992	K_k	0.9923	K_k
K	0	94	298	325	7.1960	52.07	484 ± 55.2	$\{k^*\}$	461 ± 1	$\{\eta_0\}$	918 ± 2.5	$\{\tau_d\}$
	10	99	165	185	3.2612	35.65	0.44 ± 0.03	n	0.45 ± 0.03	n	9 ± 0.037	$\{k^*\}$
	20	100	161	165	12.3802	46.22	0.9970	K_k	0.9967	K_k	0.9863	K_k

Table 4. Results of Sheetfed Inks Rapida Flow Curve Segmentation, Thixotropy Measurement, and the Application of the Mathematical Models

Heatset inks	$w(\text{water})$	D_{\min}	D_{\max}	D_{crit}	A	$\eta(D = 120 \text{ s}^{-1})$	Ostwald	$\{P\}$	Logarithm	$\{P\}$	Casson	$\{P\}$
	%	s^{-1}	s^{-1}	s^{-1}	$\text{Pa s}^{-1} 10^{-4}$	Pa s						
C	0	27	140	162	8.7524	51.96	55 ± 9	$\{k^*\}$	60 ± 1	$\{\eta_0\}$	31.4 ± 5.02	$\{\tau_d\}$
	10	27	129	136	11.2985	46.41	0.93 ± 0.03	n	0.91 ± 0.04	n	32 ± 0.046	$\{k^*\}$
	20	27	80	108	11.3673	51.52	0.9994	K_k	0.9994	K_k	0.9965	K_k
M	0	18	66	83	11.3602	71.75	126 ± 12	$\{k^*\}$	123 ± 1	$\{\eta_0\}$	29.4 ± 1.09	$\{\tau_d\}$
	10	18	63	74	11.6214	53.19	0.88 ± 0.03	n	0.88 ± 0.02	n	65 ± 0.034	$\{k^*\}$
	20	18	54	82	8.3159	55.08	0.9913	K_k	0.9754	K_k	0.9446	K_k
Y	0	15	220	240	2.2124	43.21	45 ± 4	$\{k^*\}$	44 ± 1	$\{\eta_0\}$	11.2 ± 1.71	$\{\tau_d\}$
	10	15	210	210	0.5655	33.43	0.95 ± 0.02	n	0.95 ± 0.02	n	32 ± 0.013	$\{k^*\}$
	20	15	136	152	10.3643	37.32	0.9995	K_k	0.9995	K_k	0.9969	K_k
K	0	15	71	83	15.2007	76.69	206 ± 16	$\{k^*\}$	203 ± 1	$\{\eta_0\}$	146 ± 0.86	$\{\tau_d\}$
	10	15	77	83	12.9714	57.57	0.77 ± 0.02	n	0.78 ± 0.02	n	57 ± 0.028	$\{k^*\}$
	20	15	75	83	10.7690	63.97	0.9911	K_k	0.9889	K_k	0.9568	K_k

viscoelasticity. The range of ΔD declines with increasing of water content. Even the reproducibility of measurements was worse.

An application of mathematical models is the best way to describe the rheological properties of the inks in their complexity due to the ability to characterize a flow behaviour through specific model parameters.

Mathematical models allow to describe different relations from the rheological measurements such as η vs. D , τ vs. D , η vs. T . A suitable mathematical model ought to have some basic properties [10]:

1. It should give an accurate fit of experimental data over a wide range of shear rates.
2. It should involve a minimum number of independent constants.
3. The appropriate constants should be readily evaluated.

4. The constants should have a real physical significance.

The demand of a good correspondence of the model with experimental data could be satisfied not only by the choosing of a suitable model but even by selection of a correct part of the flow curve. In our case the correct part is defined within the range of D_{\min} – D_{\max} (*i.e.* ΔD_{opt}), because it is the only stable and reproducible part of the measured curves. Choosing the limited region D_{\min} – D_{\max} , the application of a model becomes more clear and simple.

In this work we have used three mathematical models (Figs. 4–6) described above.

As for availability of the used mathematical models we can state that their agreement with the measured data in the limited interval ΔD_{opt} is very good. However, if we try to use them in wider scale of D the

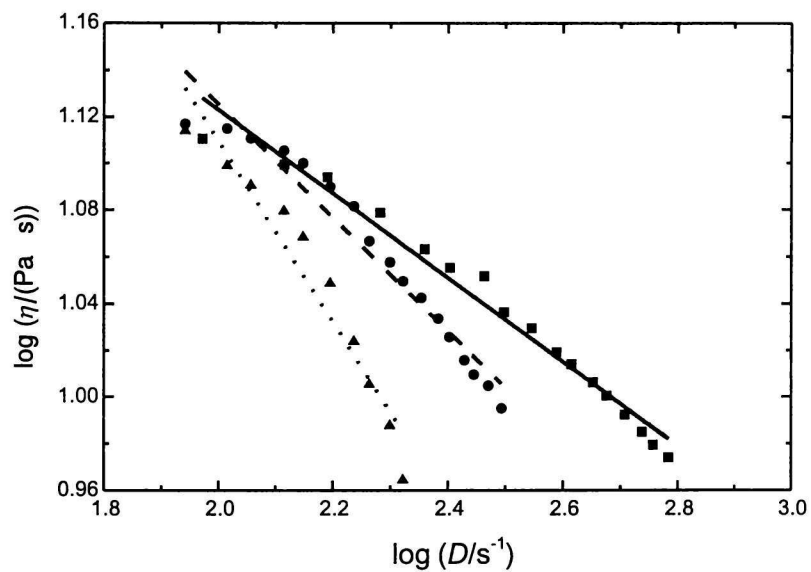


Fig. 4. Logarithmic model applied to a viscosity curve of yellow newsink (—) and its 10 mass % (---) and 20 mass % (···) emulsions.

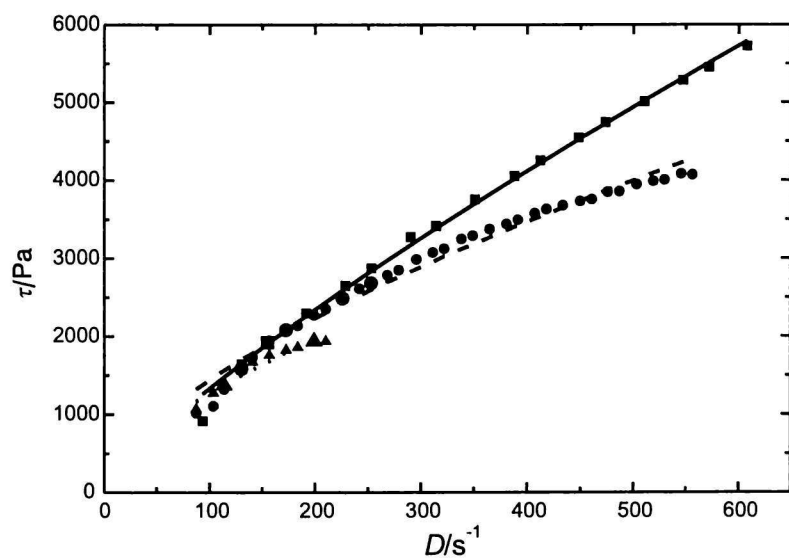


Fig. 5. Ostwald model applied to a flow curve of yellow newsink (—) and its 10 mass % (---) and 20 mass % (···) emulsions.

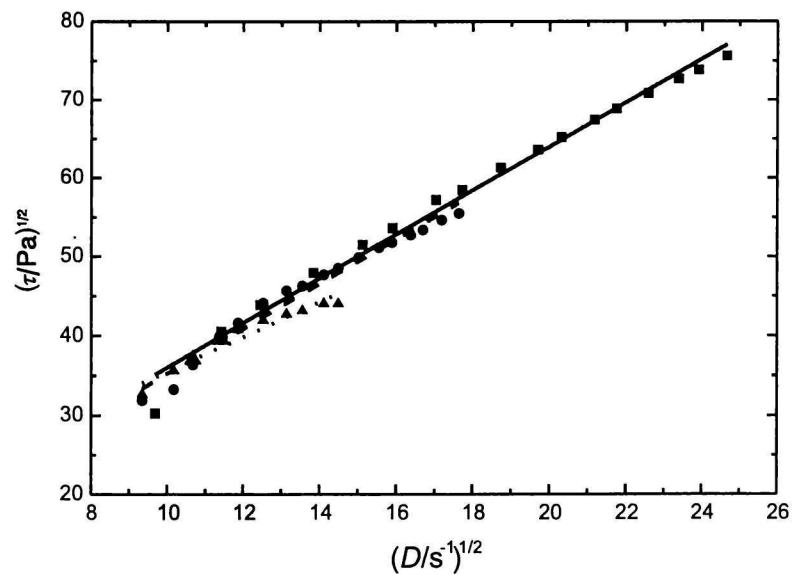


Fig. 6. Casson model applied to a flow curve of yellow newsink (—) and its 10 mass % (---) and 20 mass % (···) emulsions.

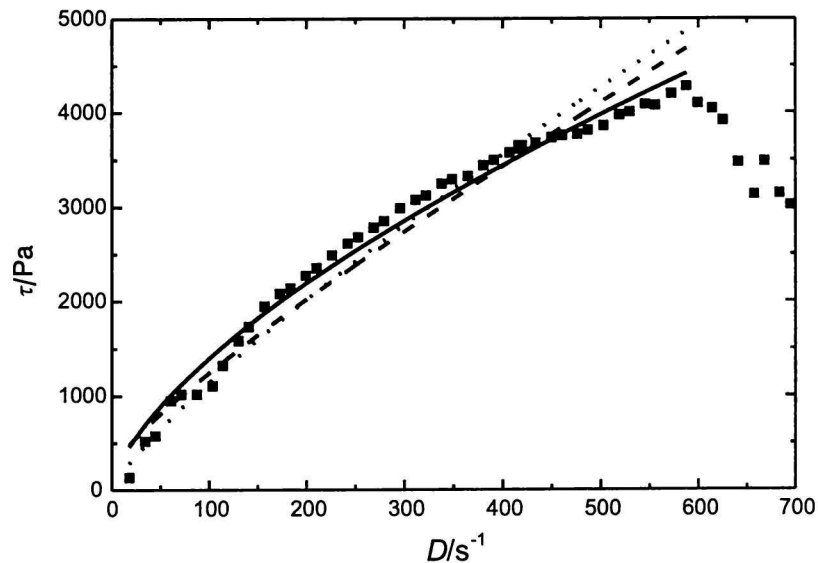


Fig. 7. Comparison of the used mathematical models (Ostwald model (—), Casson model (---), and logarithmic model (···)) applied to a 10 mass % emulsion flow curve of yellow newsink (Casson and logarithmic model are recounted to a relation: $\tau = f(D)$).

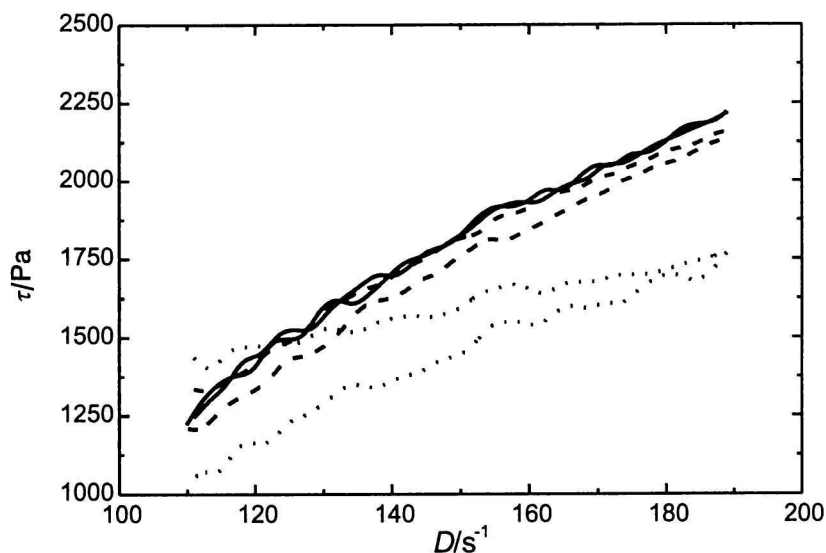


Fig. 8. Thixotropic curves of yellow newsink (—) and its 10 mass % (---) and 20 mass % (···) emulsions.

most available seems to be the Ostwald model for its slow tendency to reach steady course (provided by n parameter, Fig. 7). This model has the highest predictability in the regions outside the ΔD_{opt} interval.

Thixotropy is a phenomenon of time-dependent rheology, when viscosity is time-decreasing under constant shear rate. This phenomenon is caused by interactions of ink components (such as vehicle system, dye particles).

As well as measurement of flow curves is recommended for the limited range of shear rates (D_{min} to D_{max}), also the thixotropy measurements need to be performed in exactly defined and reproducible range, *i.e.* between D_{min} and D_{max} .

The rate of thixotropy was increasing by water content raising. If the thixotropy measurement exceeds D_{max} , the increase of thixotropy loop area is to be expected (see Figs. 8, 9).

It is well known that the hysteresis loop area is a measurement of the ability of the ink structure to recover when the shear rate decreases during down curve measurement. The large hysteresis loop area is an indication of loss of structure recovery. The larger the area, the slower the rate of structure recovery, and *vice versa*.

As we can see in Tables 1—4, the higher loop area values were observed in the case of sheetfed inks Rapida and Reflecta. On the other hand, the lower loop area was observed and higher rate of emulsion stability could be expected in the case of newsinks and heatset inks.

CONCLUSION

The rheological properties of four types of process offset inks were studied in pure forms, and in emul-

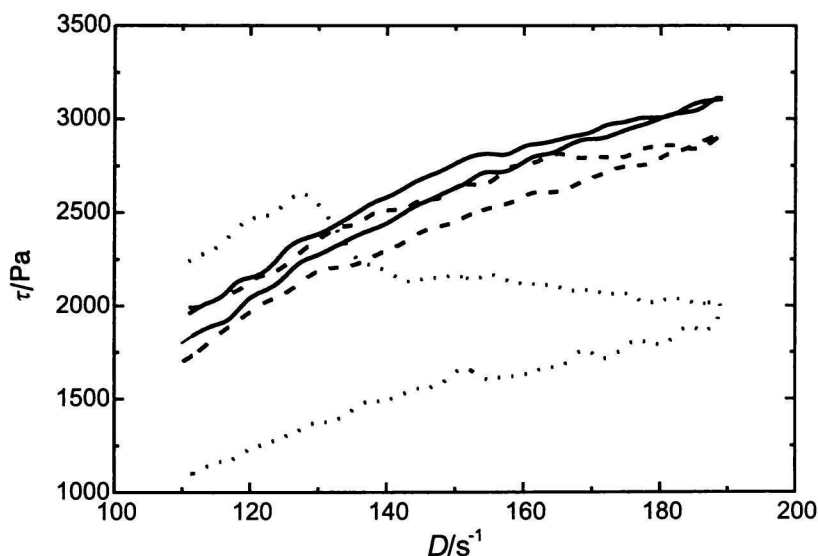


Fig. 9. Thixotropic curves of black newsink (—) and its 10 mass % (---) and 20 mass % (···) emulsions.

sions with 10 mass % and 20 mass % content of water. All systems have shown properties typical for pseudoplastic non-Newtonian fluids with viscosity decreasing along shear rate (shear-thinning behaviour). The inks have shown viscoelastic behaviour characterized by remounting of ink from measuring gap when specific values of shear rate D_{crit} and critical shear stress τ_{crit} were achieved. The value of D_{crit} was not the same for different inks in one ink set, and it decreases with increasing ink consistency as well as with raising water content. When the value of τ_{crit} was exceeded, the measurements have lost reproducibility and information from this region was valueless for ink properties evaluation. The optimal measuring interval ΔD_{opt} was defined to obtain reproducible results.

As for availability of the used mathematical models, the suitable one is the Ostwald model due to its ability of data extrapolation over the ΔD_{opt} interval.

The heatset inks are very viscous fluids suitable for very high speed printing and they appear to be more viscous than newsinks. As for the special arrangement of Rapida sheetfed inks, which were produced for even higher printing speed, they are more viscous than the heatset inks (see tables). The same trend is typical in accordance with the expectations for logarithmic model parameter η_0 .

Acknowledgements. This study was supported by the Slovak Scientific Grant Agency VEGA and the Ministry of Education of the Slovak Republic, Grant No. 1/6156/99.

REFERENCES

1. Durand, R. R., Jr. and Wasilewski, O., *Technical Association of the Graphic Arts Proceedings*, p. 339. Rochester, NY, 1991.
2. Surland, A., *Technical Association of the Graphic Arts Proceedings*, p. 191. Rochester, NY, 1983.
3. Surland, A., *Technical Association of the Graphic Arts Proceedings*, p. 222. Rochester, NY, 1980.
4. Chou, S. M. and Cher, M., *Technical Association of the Graphic Arts Proceedings*, p. 257. Rochester, NY, 1989.
5. Durand, R. R., Jr. and Wasilewski, O., *Technical Association of the Graphic Arts Proceedings*, p. 285. Rochester, NY, 1993.
6. Rizk, N. Y., Leary, T. G., and Newton, J. A., *Technical Association of the Graphic Arts Proceedings*, p. 379. Rochester, NY, 1994.
7. Chou, S. M. and Fadner, T. A., *Technical Association of the Graphic Arts Proceedings*, p. 37. Rochester, NY, 1986.
8. Cerny, J., *Graphic Arts in Finland* 22, 3 (1993).
9. Blayo, A., Gandini, A., and Le Nest, J.-F., *Technical Association of the Graphic Arts Proceedings*, p. 406. Rochester, NY, 1996.
10. Cross, M. M., *J. Colloid Sci.* 20, 417 (1965).